

# Light Scalar Fields Foster Production of Primordial Black Holes

Dario L. Lorenzoni,<sup>1,2,\*</sup> Sarah R. Geller,<sup>3,4,5,†</sup> Zachary Ireland,<sup>6</sup>  
David I. Kaiser,<sup>7</sup> Evan McDonough,<sup>2</sup> and Kyle A. Wittmeier<sup>2</sup>

<sup>1</sup>*Department of Physics & Astronomy, University of Manitoba, Winnipeg, MB R3T 2N2, Canada*

<sup>2</sup>*Department of Physics, University of Winnipeg, Winnipeg, MB R3B 2E9, Canada*

<sup>3</sup>*Santa Cruz Institute for Particle Physics, Santa Cruz, CA 95064, USA*

<sup>4</sup>*Department of Physics, University of California, Santa Cruz, Santa Cruz, CA 95064, USA*

<sup>5</sup>*Physics Division, Lawrence Berkeley National Laboratory, 1 Cyclotron Road, Berkeley, CA, 94720, USA*

<sup>6</sup>*Department of Physics, University of Toronto, Toronto, ON M5S 1A7, Canada*

<sup>7</sup>*Center for Theoretical Physics, Massachusetts Institute of Technology, Cambridge, MA 02139, USA*

Scalar fields are ubiquitous in theories of high-energy physics. In the context of cosmic inflation, this suggests the existence of spectator fields, which provide a subdominant source of energy density. We show that spectator fields boost the inflationary production of primordial black holes, with single-field ultra-slow roll evolution supplanted by a phase of evolution along the spectator direction, and primordial perturbations amplified by the resulting multifield dynamics. This generic mechanism is largely free from the severe fine-tuning that afflicts single-field inflationary PBH models.

**Introduction.** Primordial black holes (PBHs) [1–7], which form from the direct collapse of overdensities rather than from stellar collapse, are a leading candidate to explain some or all of the mysterious dark matter that fills the universe [8–17]. Perhaps the most well-studied mechanism for PBH formation is the post-inflationary collapse of primordial overdensities sourced by curvature fluctuations from inflation. For example, single-field models with a potential  $V(\varphi)$  that is tuned to yield brief periods of ultra-slow-roll (USR) evolution are known to produce spikes in the curvature power spectrum [18–39]. However, demanding these models fit precision cosmic microwave background (CMB) observations [40–43] and produce a population of PBHs satisfying all known constraints [8–17] requires a significant fine-tuning of model parameters. (Following Ref. [34], by “fine-tuning” we mean that predictions for physical quantities, such as the power spectrum of gauge-invariant curvature perturbations, become exponentially sensitive to small changes in one or more model parameters.) On the other hand, multifield inflation models for PBHs have also been proposed (see, e.g., [44–56]), and in certain cases the fine-tuning can be less severe than in the single-field case [56]. Multifield models are well motivated by particle physics, e.g., the Standard Model contains four real scalar degrees of freedom, and extensions typically contain many more.

In this paper we identify a broad class of particularly simple multifield models that match CMB observations and yield a population of PBHs. These models include two minimally coupled scalar fields with a potential of the form  $V(\varphi, \chi) = V_{\text{PBH}}(\varphi) + V_{\text{S}}(\chi)$ . The inflaton potential  $V_{\text{PBH}}(\varphi)$  is characterized by a small-field feature, such as a near-inflection point, which leads to a departure from ordinary slow-roll evolution. The field  $\chi$  is a light

spectator field which does not couple directly to the inflation, and whose contribution to the total energy density remains subdominant throughout inflation. We consider the simplest potential for the spectator,  $V_{\text{S}}(\chi) = \frac{1}{2}m_{\chi}^2\chi^2$ , and study dynamics of the multifield system for various forms of  $V_{\text{PBH}}(\varphi)$  that lead to PBH formation.

By adding a simple spectator field to PBH-producing single-field models, we fundamentally change the physical mechanism by which primordial curvature perturbations become amplified. In particular, such models *do not undergo a USR phase*. Instead, curvature perturbations on scales  $k_{\text{PBH}} \gg k_{\text{CMB}}$  become amplified by *tachyonic growth of isocurvature perturbations* combined with *turns in field space*—features that have no analog in single-field models. This provides a generic mechanism [57] that is applicable to any base model in which  $V_{\text{PBH}}(\varphi)$  (when considered in a single-field context) yields a spike in the primordial curvature power spectrum. The mechanism exhibits a *resilience* that is absent in the corresponding single-field cases: the models can match CMB observations and produce an appropriate population of PBHs while alleviating the exponential sensitivity to small changes in parameters that plagues the single-field models. See Fig. 1.

**Inflationary Dynamics.** We consider two-field models governed by the action

$$S = \int d^4x \sqrt{-g} \left[ \frac{M_{\text{Pl}}^2}{2} R - \frac{1}{2}(\partial\varphi)^2 - \frac{1}{2}(\partial\chi)^2 - V(\varphi, \chi) \right], \quad (1)$$

where  $M_{\text{Pl}} \equiv 1/\sqrt{8\pi G}$  is the reduced Planck mass and  $V(\varphi, \chi) = V_{\text{PBH}}(\varphi) + V_{\text{S}}(\chi)$ , with  $V_{\text{S}}(\chi) = \frac{1}{2}m_{\chi}^2\chi^2$ . [58] The evolution of the background fields is governed by

\* Corresponding Author. [lorenzod@myumanitoba.ca](mailto:lorenzod@myumanitoba.ca)

† Corresponding Author. [sageller@ucsc.edu](mailto:sageller@ucsc.edu)

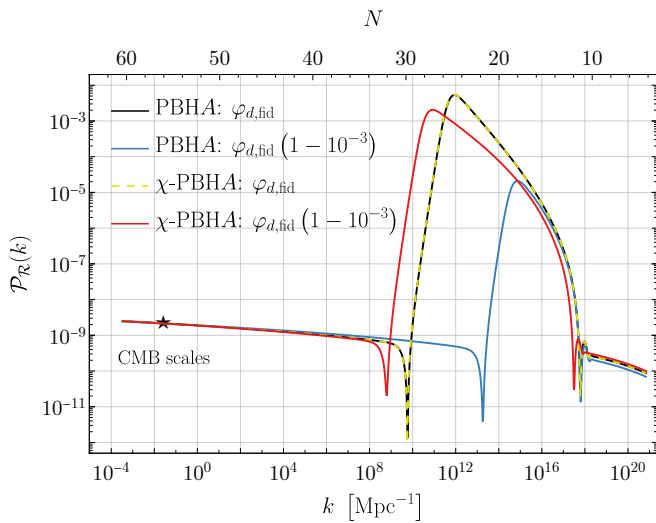


FIG. 1. Power spectra  $\mathcal{P}_{\mathcal{R}}(k)$  of primordial curvature perturbations for Model A of Eq. (10), with and without a spectator field  $\chi$ . In the single-field case, a small variation of the model parameter  $\varphi_d$  eliminates PBH production, shifting the peak of  $\mathcal{P}_{\mathcal{R}}(k)$  for fiducial values of the parameters (black curve) to far below the threshold ( $10^{-3}$ ) required for PBH production (blue curve). (Variations of  $\varphi_d$  as small as  $\mathcal{O}(10^{-5})$  yield  $\mathcal{O}(1)$  shifts in the peak of  $\mathcal{P}_{\mathcal{R}}(k)$  [34].) Upon adding the spectator  $\chi$ , the power spectrum remains resilient to the same small parameter change (yellow-dashed to red curves). Model parameters and corresponding observables are reported in Tables AI and AII.

their equations of motion and the Friedmann equation,

$$\ddot{\varphi} + 3H\dot{\varphi} = -\frac{dV_{\text{PBH}}}{d\varphi}, \quad \ddot{\chi} + 3H\dot{\chi} = -\frac{dV_{\text{S}}}{d\chi}, \quad (2)$$

$$H^2 = \frac{1}{3M_{\text{Pl}}^2} \left( \frac{\dot{\varphi}^2}{2} + \frac{\dot{\chi}^2}{2} + V_{\text{PBH}} + V_{\text{S}} \right). \quad (3)$$

Note that the inflaton field  $\varphi$  and the spectator  $\chi$  are coupled only via the Friedmann equation. In particular,  $\chi$  contributes a small increase to  $H$  and hence to the Hubble friction term for  $\varphi$ . For suitable choice of potentials, these equations admit inflationary solutions characterized by the slow-roll parameters  $\epsilon \equiv -\dot{H}/H^2$  and  $\eta \equiv 2\epsilon - \dot{\epsilon}/(2H\epsilon)$ . The decoupling of the fields implies that the first slow-roll parameter is sum-separable,

$$\epsilon = \frac{1}{2} \frac{\dot{\varphi}^2}{H^2 M_{\text{Pl}}^2} + \frac{1}{2} \frac{\dot{\chi}^2}{H^2 M_{\text{Pl}}^2} \equiv \epsilon_{\varphi} + \epsilon_{\chi}. \quad (4)$$

To study the dynamics of the two-field system we deploy the usual formalism for multifield models [59–66]. Using the notation  $\dot{\phi}^I \equiv \{\dot{\varphi}, \dot{\chi}\}$ , we may define the magnitude of the velocity of the background fields as  $\dot{\sigma} \equiv |\dot{\phi}^I| = \sqrt{\dot{\varphi}^2 + \dot{\chi}^2}$ . We can then define a field-space unit vector  $\hat{\sigma}^I \equiv \dot{\phi}^I/\dot{\sigma} = \epsilon^{-1/2} \{\sqrt{\epsilon_{\varphi}}, \sqrt{\epsilon_{\chi}}\}$  that points along the direction of the background fields' motion (the *adiabatic* direction). We also define the vec-

tor  $\hat{s}^J \equiv \epsilon^{IJ} \hat{\sigma}_I$  (the *isocurvature* direction) which is orthogonal to  $\hat{\sigma}^I$ . (Here  $\epsilon^{IJ}$  is the two-dimensional Levi-Civita antisymmetric pseudo-tensor.) The time evolution of these unit vectors is captured by the turn rate pseudovector and pseudoscalar,

$$\omega^I \equiv \partial_t \hat{\sigma}^I, \quad \omega \equiv \epsilon_{IJ} \hat{\sigma}^I \omega^J. \quad (5)$$

In the simple two-field models studied here, the turn rate is  $\omega = \dot{\theta}$ , where  $\theta$  is the angle  $\hat{\sigma}^I$  makes with the  $\varphi$ -axis.

We may also consider the gauge-invariant fluctuations along the adiabatic (or *curvature*) and isocurvature directions, and decompose them into Fourier modes denoted  $\mathcal{R}_k$  and  $\mathcal{S}_k$ , respectively [66, 67]. (We consider perturbations around a spatially flat Friedmann-Lemaître-Robertson-Walker line-element.) To linear order, these obey the coupled equations of motion [65, 68–70]

$$\frac{d}{dt} (\dot{\mathcal{R}}_k - 2\omega \mathcal{S}_k) + (3 + \delta)H (\dot{\mathcal{R}}_k - 2\omega \mathcal{S}_k) + \frac{k^2}{a^2} \mathcal{R}_k = 0, \quad (6)$$

$$\ddot{\mathcal{S}}_k + (3 + \delta)H \dot{\mathcal{S}}_k + \left( \frac{k^2}{a^2} + \mu_s^2 \right) \mathcal{S}_k = -2\omega \dot{\mathcal{R}}_k. \quad (7)$$

Here  $\delta \equiv \dot{\epsilon}/(H\epsilon) = 4\epsilon - 2\eta$  and  $\mu_s$  is the isocurvature mass [65, 68–70]

$$\mu_s^2 = M_{ss} - M_{\sigma\sigma} + 2H^2\epsilon(3 + \delta - \epsilon), \quad (8)$$

where  $M_{\sigma\sigma}$  and  $M_{ss}$  are projections of the second derivatives of  $V(\varphi, \chi)$  onto the adiabatic and isocurvature directions. The dimensionless power spectra for modes  $\mathcal{X} \in \{\mathcal{R}, \mathcal{S}\}$  are defined as  $\mathcal{P}_{\mathcal{X}}(k) \equiv k^3 |\mathcal{X}_k|^2 / (2\pi^2)$ . On super-Hubble scales ( $k/a \ll H$ ), the system vastly simplifies: the curvature and isocurvature modes satisfy

$$\dot{\mathcal{R}}_k \simeq 2\omega \mathcal{S}_k, \quad \ddot{\mathcal{S}}_k + (3 + \delta)H \dot{\mathcal{S}}_k + \tilde{\mu}_s^2 \mathcal{S}_k \simeq 0, \quad (9)$$

where the effective isocurvature mass (in the long-wavelength limit) is  $\tilde{\mu}_s^2 \equiv \mu_s^2 + 4\omega^2$ . The isocurvature modes  $\mathcal{S}_k$  will experience tachyonic growth when  $\tilde{\mu}_s^2 < 0$  and will decay when  $\tilde{\mu}_s^2 > 0$ .

**Single-Field Cases.** In single-field models, for which  $\mathcal{S}_k = 0$  and  $\omega = 0$  identically, the gauge-invariant curvature perturbations  $\mathcal{R}_k$  will become amplified on certain scales  $k_{\text{PBH}}$  because of changes in the evolution of the background field  $\varphi$ . In particular, note from Eq. (6) that the Hubble damping term,  $(3 + \delta)H\dot{\mathcal{R}}_k$ , will change sign whenever  $(3 + \delta) = (3 + 4\epsilon - 2\eta)$  becomes negative. This is exactly what happens during USR, when  $\epsilon \rightarrow 0^+$  and  $\eta \rightarrow 3$ . Then long-wavelength modes, with  $k^2/(aH)^2 < |\dot{\mathcal{R}}_k/(H\dot{\mathcal{R}}_k)|$ , will become *anti-damped* and grow quasi-exponentially whenever  $\epsilon \ll 1$  and  $\eta \geq 3/2$  [18–23, 55, 56].

Single-field models will enter a USR phase when the derivative of the potential becomes nearly flat,  $\partial_{\varphi} V_{\text{PBH}}(\varphi) \sim 0$ , in the vicinity of which  $\varphi(t)$  will evolve

as  $\ddot{\varphi} \simeq -3H\dot{\varphi}$  [18, 19, 55, 56]. Whereas it is usually straightforward to arrange the functional form of  $V_{\text{PBH}}(\varphi)$  to include some portion for which  $\partial_\varphi V_{\text{PBH}}(\varphi) \sim 0$ , requiring that the system does not *remain* in USR arbitrarily long while also ensuring that the small-field feature within  $V_{\text{PBH}}(\varphi)$  does not distort predictions for CMB observables on scales  $k_{\text{CMB}}$  necessarily entails significant fine-tuning [34].

For concreteness, we consider two different forms of  $V_{\text{PBH}}(\varphi)$  which have been well-studied in the literature:

$$V_{\text{PBH},A}(\varphi) = V_0 \frac{\varphi^2}{\varphi^2 + M^2} \left( 1 + A e^{-(\varphi - \varphi_a)^2 / \sigma^2} \right), \quad (10)$$

$$V_{\text{PBH},B}(\varphi) = \frac{M_{\text{Pl}}^4 \lambda v^4 x^2 (6 - 4ax + 3x^2)}{12 (M_{\text{Pl}}^2 + bx^2)^2}, \quad (11)$$

with  $x \equiv \varphi/v$ . Model A [30] superimposes a local Gaussian “bump” on the well-known KKL $T$  potential [71]. Model B [21, 22] adds a cubic term to a potential akin to Higgs inflation [72] to engineer a quasi-inflection point. Consistent with Ref. [34], we find that small variations of model parameters, of  $\mathcal{O}(10^{-5})$  in Model A, alter the peak amplitude of the power spectrum by  $\mathcal{O}(1)$ . Moreover, parameter variations of  $\mathcal{O}(10^{-3})$  sufficiently alter the growth of modes  $\mathcal{R}_k$  such that  $\mathcal{P}_{\mathcal{R}}(k)$  never exceeds the required threshold for PBH formation. See Figs. 1 and 4 and Tables AI and AIII.

**Role of the Spectator Field.** Fig. 2 shows  $\epsilon$  and  $\omega$  for the system  $V(\varphi, \chi) = V_{\text{PBH},A}(\varphi) + V_{\text{S}}(\chi)$ . Much as in the single-field version of this model (setting  $\chi = 0$ ), the slow-roll parameter  $\epsilon_\varphi$  becomes anomalously small,  $\epsilon_\varphi \sim \mathcal{O}(10^{-10})$ , as  $\varphi$  encounters the region of its potential in which  $\partial_\varphi V_{\text{PBH},A}(\varphi) \sim 0$  (solid and dashed blue curves of Fig. 2, top panel). Yet in the two-field case, since  $V_{\text{S}}(\chi)$  has no special features,  $\chi$  never departs from ordinary slow-roll, with  $\epsilon_\chi \sim \mathcal{O}(10^{-4})$  throughout inflation (red curve). Hence  $\epsilon \geq \epsilon_\chi$  never becomes anomalously small, and the system never enters USR. (We have also confirmed that  $\eta < 3$  throughout inflation.) Meanwhile,  $\chi$  backreacts on  $\varphi$  via its contribution to  $H$ , increasing Hubble friction and lengthening the duration of phase II compared to the USR phase in the single-field case.

The fact that  $\epsilon_\chi$  never departs from ordinary slow-roll forces the system to undergo two turns. Recall that  $\hat{\sigma}^I = \epsilon^{-1/2} \{ \sqrt{\epsilon_\varphi}, \sqrt{\epsilon_\chi} \}$ ; the direction of the system’s evolution through field space depends on the ratio of  $\epsilon_\varphi$  to  $\epsilon_\chi$  over time. During phase I,  $\epsilon_\varphi > \epsilon_\chi$ , and the system predominantly evolves along the  $\varphi$  direction. Once  $\epsilon_\varphi$  begins to fall exponentially, suddenly  $\epsilon_\chi \gg \epsilon_\varphi$ , and the unit vector  $\hat{\sigma}^I$  rapidly turns to point along the  $\chi$  direction. By construction, the inflaton  $\varphi$  must eventually “escape” the flat region and reach the global minimum of  $V_{\text{PBH},A}(\varphi)$ ; this requires that  $\varphi$  roll down from a local maximum, at which  $\partial_\varphi^2 V_{\text{PBH},A}(\varphi) < 0$ . As  $\varphi$  accelerates,  $\epsilon_\varphi$  grows and eventually exceeds  $\epsilon_\chi$ , causing a second sharp turn into phase III.

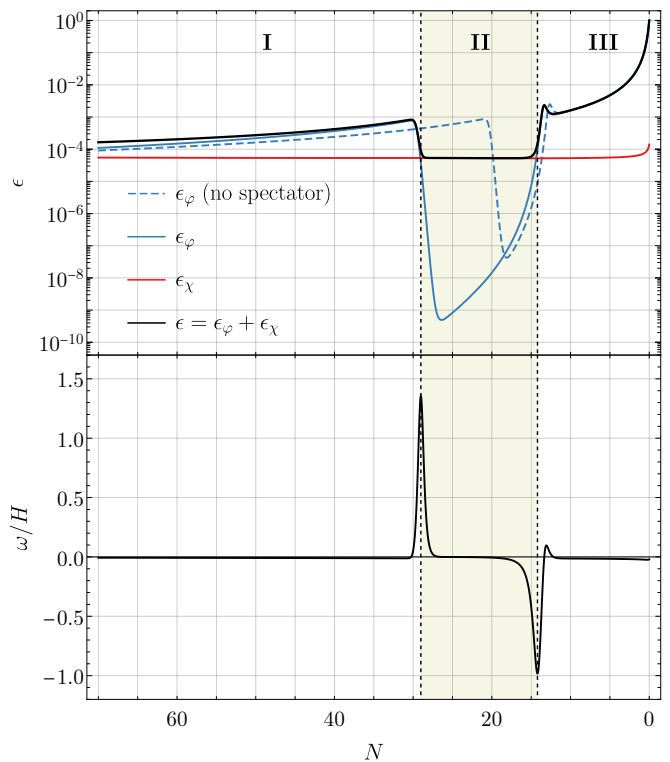


FIG. 2. Evolution of  $\epsilon$  and  $\omega$  as functions of the number of e-folds  $N$  before the end of inflation, for  $V = V_{\text{PBH},A}(\varphi) + V_{\text{S}}(\chi)$  of Eq. (10). *Top panel:* Slow-roll parameter  $\epsilon$  and its components; for comparison, the evolution of  $\epsilon_\varphi$  for the spectator-less case is also shown. *Bottom panel:* Turn rate pseudoscalar  $\omega/H$ , showing the change in trajectory of the background field system; the dashed vertical lines correspond to the extrema of  $\omega$ . *Both panels:* The highlighted ‘phase II’ is delimited by the turns; during this time,  $\epsilon_\chi \gg \epsilon_\varphi$ . Model parameters are reported in Table AI.

This pattern—two turns bracketing a phase II during which  $\epsilon_\chi \gg \epsilon_\varphi$ —is *generic* for models of the form  $V(\varphi, \chi) = V_{\text{PBH}}(\varphi) + V_{\text{S}}(\chi)$ , in which  $V_{\text{PBH}}(\varphi)$  includes features that drive a USR phase in the single-field case and  $\chi$  is a light spectator field. Regardless of the particular form that  $V_{\text{PBH}}(\varphi)$  takes, it must include some region with  $\partial_\varphi V_{\text{PBH}}(\varphi) \sim 0$  and a neighboring region in which  $\partial_\varphi^2 V_{\text{PBH}}(\varphi) < 0$ , in order for  $\varphi$  to enter and later exit a USR phase. For example, Fig. A1 shows the same three-phase structure for  $V(\varphi, \chi) = V_{\text{PBH},B}(\varphi) + V_{\text{S}}(\chi)$ , even though  $V_{\text{PBH},A}(\varphi)$  and  $V_{\text{PBH},B}(\varphi)$  in Eqs. (10)–(11) differ considerably in functional form.

The three-phase pattern of background dynamics has dramatic consequences for the evolution of the perturbations  $\mathcal{R}_k$  and  $\mathcal{S}_k$ . As shown in Eqs. (6)–(7), the curvature and isocurvature modes couple only when  $\omega \neq 0$ . Moreover, for the models in the class we consider here, during phase II the isocurvature mass  $\mu_s^2$  generically becomes tachyonic. Following the first turn, when  $\epsilon_\chi \gg \epsilon_\varphi$ , the adiabatic direction (temporarily) aligns along the  $\chi$

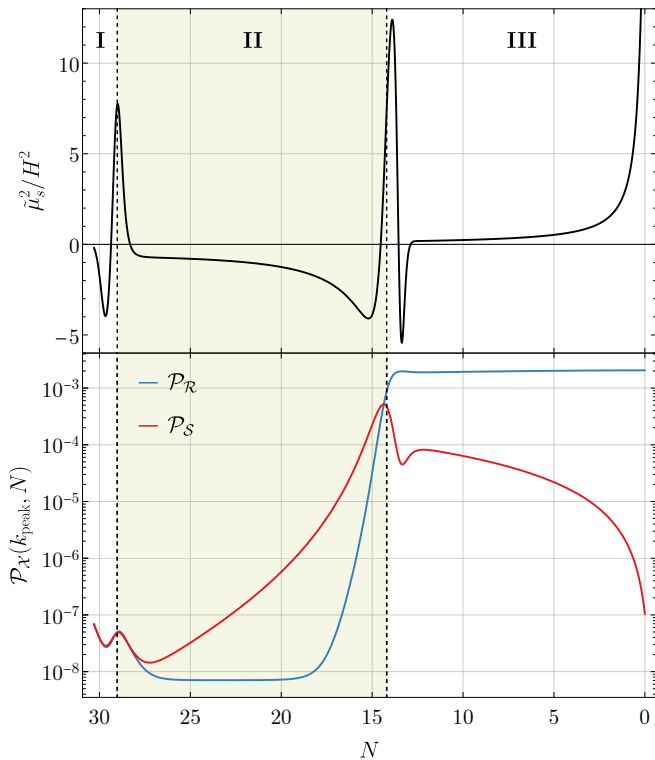


FIG. 3. Evolution of the perturbations as functions of the number of e-folds  $N$  before the end of inflation, for  $V = V_{\text{PBH},A}(\varphi) + V_S(\chi)$  of Eq. (10). *Top panel*: Isocurvature effective mass  $\tilde{\mu}_s^2$ ; the tachyonic instability is highlighted in phase II. *Bottom panel*: Spectra of curvature ( $\mathcal{R}$ ) and isocurvature ( $\mathcal{S}$ ) perturbations for a mode  $k_{\text{peak}}$  that exits the Hubble radius  $\sim 30$  e-folds before the end of inflation. The mode  $\mathcal{S}_{k_{\text{peak}}}$  is amplified exponentially via tachyonic growth while  $\tilde{\mu}_s^2 < 0$ , and transfers that power to  $\mathcal{R}_{k_{\text{peak}}}$  at the second turn, which leads to phase III. Model parameters are listed in Table AI.

direction, and hence the isocurvature direction points in the  $\varphi$  direction. During phase II, then, every term within Eq. (8) becomes negative:  $\mathcal{M}_{ss} \rightarrow \partial_\varphi^2 V_{\text{PBH}}(\varphi)$ ;  $\mathcal{M}_{\sigma\sigma} \rightarrow \partial_\chi^2 V_S(\chi)$ ; and  $(3 + \delta - \epsilon) \rightarrow (3 - 2\eta) < 0$  for  $\eta > 3/2$ . As described above, during phase II the inflaton potential *must* become concave, with  $\partial_\varphi^2 V_{\text{PBH}}(\varphi) < 0$ ; and  $\partial_\chi^2 V_S(\chi) = m_\chi^2 > 0$  always. Hence—aside from the brief periods surrounding each sharp turn, when  $\omega^2 \gg H^2$ —both  $\mu_s^2 < 0$  and  $\tilde{\mu}_s^2 < 0$  for most of phase II. (See Fig. 3, top panel.)

This phase of tachyonic instability drives rapid growth in the isocurvature modes  $\mathcal{S}_k$ . When the system encounters the second turn (onset of phase III), the now-large modes  $\mathcal{S}_k$  transfer their power to curvature perturbations  $\mathcal{R}_k$  and rapidly decay (since  $\tilde{\mu}_s^2 > 0$  in phase III), yielding an exponential increase of  $\mathcal{P}_{\mathcal{R}}(k_{\text{PBH}})$  for comoving wavenumbers  $k_{\text{PBH}}$  that were subject to the tachyonic growth. (See Fig. 3, bottom panel.) [73]

**Sensitivity to small parameter changes.** Single-field models that produce PBHs via a phase of USR re-

quire substantial fine-tuning if they are also to maintain a close match to CMB observations [34]. This is clear in Figs. 1 for  $V_{\text{PBH},A}(\varphi)$  and 4 for  $V_{\text{PBH},B}(\varphi)$ . In each case, a selection of fiducial parameters (black curves) yields power spectra  $\mathcal{P}_{\mathcal{R}}(k)$  that are in close agreement with CMB measurements and also yield PBHs with masses in the so-called asteroid-mass range,  $10^{17} \text{ g} \leq M_{\text{PBH}} \leq 10^{23} \text{ g}$ , which would be viable candidates for most or all of dark matter [8–17]. (See Tables AII and AIV.) However, a tiny variation of  $\mathcal{O}(10^{-3})$  in  $\varphi_d$  (for Model A) or  $v$  (for Model B) changes the location and peak of  $\mathcal{P}_{\mathcal{R}}(k)$  considerably (blue curves)—such that, in each case,  $\mathcal{P}_{\mathcal{R}}(k) \ll 10^{-3}$ , remaining well below the threshold required to induce gravitational collapse and produce PBHs [14, 74–78].

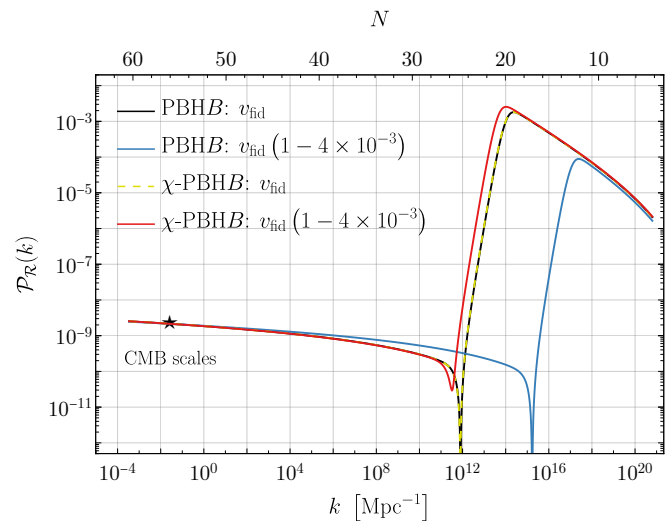


FIG. 4. Power spectra  $\mathcal{P}_{\mathcal{R}}(k)$  of primordial curvature perturbations for Model B of Eq. (11), with and without a spectator field  $\chi$ . Model parameters and corresponding observables are reported in Tables AIII and AIV.

Including a simple light spectator  $\chi$  relaxes this problem. For each model, we first find non-fine-tuned values for the spectator parameters  $m_\chi$  and  $\chi_i$  that reproduce the original single-field spectra with fiducial values of parameters in  $V_{\text{PBH}}(\varphi)$  (yellow-dashed curves in Figs. 1 and 4). We then find that a change of  $\mathcal{O}(10^{-3})$  in a fiducial parameter of  $V_{\text{PBH}}(\varphi)$  is compensated by a coarse-grained  $\mathcal{O}(1)$  variation in  $m_\chi$  and  $\chi_i$  (red curves in Figs. 1 and 4). In each case involving the spectator field, predictions for CMB observables and for PBHs relevant for dark matter remain in strong agreement with CMB measurements [40–43] and PBH constraints [8–17]. This is accomplished without overfitting: models such as  $V_{\text{PBH},B}(\varphi) + V_S(\chi)$  match eight observables ( $A_s, n_s, \alpha_s, r, \beta_{\text{iso}}, f_{\text{NL}}, \mathcal{P}_{\mathcal{R}}(k_{\text{peak}}), M_{\text{PBH}}$ )—each defined explicitly in the Appendix—using only six free parameters ( $\lambda, v, a, b, m_\chi, \chi_i$ ).

We may easily estimate the range of spectator param-

eters that are relevant for the mechanism. We require  $\epsilon_\chi > \epsilon_\varphi$  during phase II. From Eqs. (2) and (4), we find  $\epsilon_\chi = \frac{1}{18}(\chi_i/M_{\text{Pl}})^2(m_\chi/H)^4$ . Taking  $\epsilon_\varphi \sim \mathcal{O}(10^{-10})$  during USR and considering  $\chi_i$  comparable to  $\varphi_i$ , we estimate  $10^{-3} \lesssim m_\chi/H \ll 1$ , where the upper bound is required for  $\chi$  to be a light spectator.

**Discussion.** Spectator fields are a generic prediction of high energy physics, arising already in the context of the Standard Model. In this letter we have shown that in simple scenarios that include at least one light spectator field in addition to the inflaton, multifield dynamics will *generically* amplify modes  $\mathcal{R}_k$ . The background fields will undergo *turns* in field space as the system evolves toward the global minimum of the potential. Between those turns, certain modes  $k$  of the gauge-invariant isocurvature perturbations  $\mathcal{S}_k$  will grow via *tachyonic instability*, and then *transfer power* to the curvature perturbations  $\mathcal{R}_k$  before the end of inflation. Simple models involving at least one spectator field can match all CMB observables to high precision and produce a population of PBHs relevant for dark matter, while remaining resilient to small changes in model parameters.

Finally, we note that since the system of inflaton plus spectator never enters USR—and hence neither slow-roll parameter ever becomes anomalously small—it is likely that such two-field models avoid any dangerous growth of loop corrections that some have argued could threaten perturbative control for single-field USR models. (Compare Refs. [79–84] with [85–95].) Possible roles of loop corrections or other nonperturbative effects [96–98] remain the subject for further research.

**Acknowledgements.** The authors thank Josu Aurekoetxea, Bryce Cyr, Alexandra Klipfel, Jerome Martin, Sebastien Renaux-Petel, Vincent Vennin, and Rainer Weiss for helpful discussions. Portions of this research were conducted in MIT’s Center for Theoretical Physics and supported in part by the U.S. Department of Energy under Contract No. DE-SC0012567. E.M. is supported in part by a Discovery Grant from the Natural Sciences and Engineering Research Council of Canada, and by a New Investigator Operating Grant from Research Manitoba. S.R.G. is supported by the NSF Mathematical and Physical Sciences Ascending postdoctoral fellowship, under Award No. 2317018.

- 
- [1] I. D. Zel’dovich, Ya.B.; Novikov, “The Hypothesis of Cores Retarded during Expansion and the Hot Cosmological Model,” *Soviet Astron. AJ (Engl. Transl. )*, **10**, 602 (1967).
  - [2] Stephen Hawking, “Gravitationally collapsed objects of very low mass,” *Mon. Not. Roy. Astron. Soc.* **152**, 75 (1971).
  - [3] Bernard J. Carr and S. W. Hawking, “Black holes in

- the early Universe,” *Mon. Not. Roy. Astron. Soc.* **168**, 399–415 (1974).
- [4] P. Meszaros, “The behaviour of point masses in an expanding cosmological substratum,” *Astron. Astrophys.* **37**, 225–228 (1974).
- [5] Bernard J. Carr, “The Primordial black hole mass spectrum,” *Astrophys. J.* **201**, 1–19 (1975).
- [6] M. Khlopov, B. A. Malomed, and Ia. B. Zeldovich, “Gravitational instability of scalar fields and formation of primordial black holes,” *Mon. Not. Roy. Astron. Soc.* **215**, 575–589 (1985).
- [7] Jens C. Niemeyer and K. Jedamzik, “Dynamics of primordial black hole formation,” *Phys. Rev. D* **59**, 124013 (1999), [arXiv:astro-ph/9901292](#).
- [8] Maxim Yu. Khlopov, “Primordial Black Holes,” *Res. Astron. Astrophys.* **10**, 495–528 (2010), [arXiv:0801.0116 \[astro-ph\]](#).
- [9] B. J. Carr, Kazunori Kohri, Yuuiti Sendouda, and Jun’ichi Yokoyama, “New cosmological constraints on primordial black holes,” *Phys. Rev. D* **81**, 104019 (2010), [arXiv:0912.5297 \[astro-ph.CO\]](#).
- [10] Misao Sasaki, Teruaki Suyama, Takahiro Tanaka, and Shuichiro Yokoyama, “Primordial black holes—perspectives in gravitational wave astronomy,” *Class. Quant. Grav.* **35**, 063001 (2018), [arXiv:1801.05235 \[astro-ph.CO\]](#).
- [11] Bernard Carr, Kazunori Kohri, Yuuiti Sendouda, and Jun’ichi Yokoyama, “Constraints on primordial black holes,” *Rept. Prog. Phys.* **84**, 116902 (2021), [arXiv:2002.12778 \[astro-ph.CO\]](#).
- [12] Bernard Carr and Florian Kühnel, “Primordial Black Holes as Dark Matter: Recent Developments,” *Ann. Rev. Nucl. Part. Sci.* **70**, 355–394 (2020), [arXiv:2006.02838 \[astro-ph.CO\]](#).
- [13] Anne M. Green and Bradley J. Kavanagh, “Primordial Black Holes as a dark matter candidate,” *J. Phys. G* **48**, 043001 (2021), [arXiv:2007.10722 \[astro-ph.CO\]](#).
- [14] Albert Escrivà, “PBH Formation from Spherically Symmetric Hydrodynamical Perturbations: A Review,” *Universe* **8**, 66 (2022), [arXiv:2111.12693 \[gr-qc\]](#).
- [15] Pablo Villanueva-Domingo, Olga Mena, and Sergio Palomares-Ruiz, “A brief review on primordial black holes as dark matter,” *Front. Astron. Space Sci.* **8**, 87 (2021), [arXiv:2103.12087 \[astro-ph.CO\]](#).
- [16] Albert Escrivà, Florian Kühnel, and Yuichiro Tada, “Primordial Black Holes,” (2022), [arXiv:2211.05767 \[astro-ph.CO\]](#).
- [17] Matthew Gorton and Anne M. Green, “How open is the asteroid-mass primordial black hole window?” *SciPost Phys.* **17**, 032 (2024), [arXiv:2403.03839 \[astro-ph.CO\]](#).
- [18] William H. Kinney, “Horizon crossing and inflation with large eta,” *Phys. Rev. D* **72**, 023515 (2005), [arXiv:gr-qc/0503017](#).
- [19] Jerome Martin, Hayato Motohashi, and Teruaki Suyama, “Ultra Slow-Roll Inflation and the non-Gaussianity Consistency Relation,” *Phys. Rev. D* **87**, 023514 (2013), [arXiv:1211.0083 \[astro-ph.CO\]](#).
- [20] Jose Maria Ezquiaga, Juan Garcia-Bellido, and Ester Ruiz Morales, “Primordial Black Hole production in Critical Higgs Inflation,” *Phys. Lett. B* **776**, 345–349 (2018), [arXiv:1705.04861 \[astro-ph.CO\]](#).
- [21] Juan Garcia-Bellido and Ester Ruiz Morales, “Primordial black holes from single field models of inflation,” *Phys. Dark Univ.* **18**, 47–54 (2017), [arXiv:1702.03901](#)

- [astro-ph.CO].
- [22] Cristiano Germani and Tomislav Prokopec, “On primordial black holes from an inflection point,” *Phys. Dark Univ.* **18**, 6–10 (2017), arXiv:1706.04226 [astro-ph.CO].
- [23] Kristjan Kannike, Luca Marzola, Martti Raidal, and Hardi Veermäe, “Single Field Double Inflation and Primordial Black Holes,” *JCAP* **09**, 020 (2017), arXiv:1705.06225 [astro-ph.CO].
- [24] Hayato Motohashi and Wayne Hu, “Primordial Black Holes and Slow-Roll Violation,” *Phys. Rev. D* **96**, 063503 (2017), arXiv:1706.06784 [astro-ph.CO].
- [25] Haoran Di and Yungui Gong, “Primordial black holes and second order gravitational waves from ultra-slow-roll inflation,” *JCAP* **07**, 007 (2018), arXiv:1707.09578 [astro-ph.CO].
- [26] Guillermo Ballesteros and Marco Taoso, “Primordial black hole dark matter from single field inflation,” *Phys. Rev. D* **97**, 023501 (2018), arXiv:1709.05565 [hep-ph].
- [27] Chris Pattison, Vincent Vennin, Hooshyar Assadollahi, and David Wands, “Quantum diffusion during inflation and primordial black holes,” *JCAP* **10**, 046 (2017), arXiv:1707.00537 [hep-th].
- [28] Samuel Passaglia, Wayne Hu, and Hayato Motohashi, “Primordial black holes and local non-Gaussianity in canonical inflation,” *Phys. Rev. D* **99**, 043536 (2019), arXiv:1812.08243 [astro-ph.CO].
- [29] Matteo Biagetti, Gabriele Franciolini, Alex Kehagias, and Antonio Riotto, “Primordial Black Holes from Inflation and Quantum Diffusion,” *JCAP* **07**, 032 (2018), arXiv:1804.07124 [astro-ph.CO].
- [30] Swagat S. Mishra and Varun Sahni, “Primordial Black Holes from a tiny bump/dip in the Inflation potential,” *JCAP* **04**, 007 (2020), arXiv:1911.00057 [gr-qc].
- [31] Daniel G. Figueroa, Sami Raatikainen, Syksy Rasanen, and Eemeli Tomberg, “Non-Gaussian Tail of the Curvature Perturbation in Stochastic Ultraslow-Roll Inflation: Implications for Primordial Black Hole Production,” *Phys. Rev. Lett.* **127**, 101302 (2021), arXiv:2012.06551 [astro-ph.CO].
- [32] Alexandros Karam, Niko Koivunen, Eemeli Tomberg, Ville Vaskonen, and Hardi Veermäe, “Anatomy of single-field inflationary models for primordial black holes,” *JCAP* **03**, 013 (2023), arXiv:2205.13540 [astro-ph.CO].
- [33] Ogan Özsoy and Gianmassimo Tasinato, “Inflation and Primordial Black Holes,” *Universe* **9**, 203 (2023), arXiv:2301.03600 [astro-ph.CO].
- [34] Philippa S. Cole, Andrew D. Gow, Christian T. Byrnes, and Subodh P. Patil, “Primordial black holes from single-field inflation: a fine-tuning audit,” *JCAP* **08**, 031 (2023), arXiv:2304.01997 [astro-ph.CO].
- [35] Michele Cicoli, Victor A. Diaz, and Francisco G. Pedro, “Primordial Black Holes from String Inflation,” *JCAP* **06**, 034 (2018), arXiv:1803.02837 [hep-th].
- [36] Michele Cicoli, Francisco G. Pedro, and Nicola Pedron, “Secondary GWs and PBHs in string inflation: formation and detectability,” *JCAP* **08**, 030 (2022), arXiv:2203.00021 [hep-th].
- [37] Yi-Fu Cai, Xiao-Han Ma, Misao Sasaki, Dong-Gang Wang, and Zihan Zhou, “Highly non-Gaussian tails and primordial black holes from single-field inflation,” *JCAP* **12**, 034 (2022), arXiv:2207.11910 [astro-ph.CO].
- [38] Keisuke Inomata, Evan McDonough, and Wayne Hu, “Primordial black holes arise when the inflaton falls,” *Phys. Rev. D* **104**, 123553 (2021), arXiv:2104.03972 [astro-ph.CO].
- [39] Keisuke Inomata, Evan McDonough, and Wayne Hu, “Amplification of primordial perturbations from the rise or fall of the inflaton,” *JCAP* **02**, 031 (2022), arXiv:2110.14641 [astro-ph.CO].
- [40] Y. Akrami *et al.* (Planck), “Planck 2018 results. IX. Constraints on primordial non-Gaussianity,” *Astron. Astrophys.* **641**, A9 (2020), arXiv:1905.05697 [astro-ph.CO].
- [41] N. Aghanim *et al.* (Planck), “Planck 2018 results. VI. Cosmological parameters,” *Astron. Astrophys.* **641**, A6 (2020), [Erratum: *Astron. Astrophys.* 652, C4 (2021)], arXiv:1807.06209 [astro-ph.CO].
- [42] Y. Akrami *et al.* (Planck), “Planck 2018 results. X. Constraints on inflation,” *Astron. Astrophys.* **641**, A10 (2020), arXiv:1807.06211 [astro-ph.CO].
- [43] P. A. R. Ade *et al.* (BICEP, Keck), “Improved Constraints on Primordial Gravitational Waves using Planck, WMAP, and BICEP/Keck Observations through the 2018 Observing Season,” *Phys. Rev. Lett.* **127**, 151301 (2021), arXiv:2110.00483 [astro-ph.CO].
- [44] Lisa Randall, Marin Soljacic, and Alan H. Guth, “Supernatural inflation: Inflation from supersymmetry with no (very) small parameters,” *Nucl. Phys. B* **472**, 377–408 (1996), arXiv:hep-ph/9512439.
- [45] Juan Garcia-Bellido, Andrei D. Linde, and David Wands, “Density perturbations and black hole formation in hybrid inflation,” *Phys. Rev. D* **54**, 6040–6058 (1996), arXiv:astro-ph/9605094.
- [46] David H. Lyth, “Contribution of the hybrid inflation waterfall to the primordial curvature perturbation,” *JCAP* **07**, 035 (2011), arXiv:1012.4617 [astro-ph.CO].
- [47] Edgar Bugaev and Peter Klimai, “Formation of primordial black holes from non-Gaussian perturbations produced in a waterfall transition,” *Phys. Rev. D* **85**, 103504 (2012), arXiv:1112.5601 [astro-ph.CO].
- [48] Illan F. Halpern, Mark P. Hertzberg, Matthew A. Joss, and Evangelos I. Sfakianakis, “A Density Spike on Astrophysical Scales from an N-Field Waterfall Transition,” *Phys. Lett. B* **748**, 132–143 (2015), arXiv:1410.1878 [astro-ph.CO].
- [49] Sébastien Clesse and Juan García-Bellido, “Massive Primordial Black Holes from Hybrid Inflation as Dark Matter and the seeds of Galaxies,” *Phys. Rev. D* **92**, 023524 (2015), arXiv:1501.07565 [astro-ph.CO].
- [50] Masahiro Kawasaki and Yuichiro Tada, “Can massive primordial black holes be produced in mild waterfall hybrid inflation?” *JCAP* **08**, 041 (2016), arXiv:1512.03515 [astro-ph.CO].
- [51] Matteo Braglia, Andrei Linde, Renata Kallosh, and Fabio Finelli, “Hybrid  $\alpha$ -attractors, primordial black holes and gravitational wave backgrounds,” *JCAP* **04**, 033 (2023), arXiv:2211.14262 [astro-ph.CO].
- [52] Jacopo Fumagalli, Sébastien Renaux-Petel, John W. Ronayne, and Lukas T. Witkowski, “Turning in the landscape: A new mechanism for generating primordial black holes,” *Phys. Lett. B* **841**, 137921 (2023), arXiv:2004.08369 [hep-th].
- [53] Matteo Braglia, Dhiraj Kumar Hazra, Fabio Finelli, George F. Smoot, L. Sriramkumar, and Alexei A. Starobinsky, “Generating PBHs and small-scale GWs in two-field models of inflation,” *JCAP* **08**, 001 (2020),

- arXiv:2005.02895 [astro-ph.CO].
- [54] Gonzalo A. Palma, Spyros Sypsas, and Cristobal Zenteno, “Seeding primordial black holes in multi-field inflation,” *Phys. Rev. Lett.* **125**, 121301 (2020), arXiv:2004.06106 [astro-ph.CO].
- [55] Sarah R. Geller, Wenzer Qin, Evan McDonough, and David I. Kaiser, “Primordial black holes from multi-field inflation with nonminimal couplings,” *Phys. Rev. D* **106**, 063535 (2022), arXiv:2205.04471 [hep-th].
- [56] Wenzer Qin, Sarah R. Geller, Shyam Balaji, Evan McDonough, and David I. Kaiser, “Planck constraints and gravitational wave forecasts for primordial black hole dark matter seeded by multifield inflation,” *Phys. Rev. D* **108**, 043508 (2023), arXiv:2303.02168 [astro-ph.CO].
- [57] Previous studies have highlighted model-dependent scenarios in which spectator fields can enhance primordial curvature perturbations, and hence PBH formation [99–103].
- [58] We define a scalar spectator field as being subdominant in potential energy density,  $|V_S/V_{\text{PBH}}|_{t_{\text{CMB}}} \ll 1$ , with no direct coupling to the inflaton, and with a sub-Hubble mass  $|m_\chi/H|_{t_{\text{CMB}}} \ll 1$ , where  $H$  is the Hubble parameter. Both conditions are evaluated at the time  $t_{\text{CMB}}$  when the comoving CMB pivot scale  $k_{\text{CMB}}$  first exits the Hubble radius.
- [59] Misao Sasaki and Ewan D. Stewart, “A General analytic formula for the spectral index of the density perturbations produced during inflation,” *Prog. Theor. Phys.* **95**, 71–78 (1996), arXiv:astro-ph/9507001.
- [60] Christopher Gordon, David Wands, Bruce A. Bassett, and Roy Maartens, “Adiabatic and entropy perturbations from inflation,” *Phys. Rev. D* **63**, 023506 (2000), arXiv:astro-ph/0009131.
- [61] David Wands, Nicola Bartolo, Sabino Matarrese, and Antonio Riotto, “An Observational test of two-field inflation,” *Phys. Rev. D* **66**, 043520 (2002), arXiv:astro-ph/0205253.
- [62] David Langlois and Sebastien Renaux-Petel, “Perturbations in generalized multi-field inflation,” *JCAP* **04**, 017 (2008), arXiv:0801.1085 [hep-th].
- [63] Courtney M. Peterson and Max Tegmark, “Testing Two-Field Inflation,” *Phys. Rev. D* **83**, 023522 (2011), arXiv:1005.4056 [astro-ph.CO].
- [64] Jinn-Ouk Gong and Takahiro Tanaka, “A covariant approach to general field space metric in multi-field inflation,” *JCAP* **03**, 015 (2011), [Erratum: *JCAP* **02**, E01 (2012)], arXiv:1101.4809 [astro-ph.CO].
- [65] David I. Kaiser, Edward A. Mazenc, and Evangelos I. Sfakianakis, “Primordial Bispectrum from Multifield Inflation with Nonminimal Couplings,” *Phys. Rev. D* **87**, 064004 (2013), arXiv:1210.7487 [astro-ph.CO].
- [66] Jinn-Ouk Gong, “Multi-field inflation and cosmological perturbations,” *Int. J. Mod. Phys. D* **26**, 1740003 (2016), arXiv:1606.06971 [gr-qc].
- [67] David Wands, “Multiple field inflation,” *Lect. Notes Phys.* **738**, 275–304 (2008), arXiv:astro-ph/0702187.
- [68] Ana Achúcarro, Vicente Atal, Cristiano Germani, and Gonzalo A. Palma, “Cumulative effects in inflation with ultra-light entropy modes,” *JCAP* **02**, 013 (2017), arXiv:1607.08609 [astro-ph.CO].
- [69] Evan McDonough, Alan H. Guth, and David I. Kaiser, “Nonminimal Couplings and the Forgotten Field of Axion Inflation,” (2020), arXiv:2010.04179 [hep-th].
- [70] Dario L. Lorenzoni, David I. Kaiser, and Evan McDonough, “Natural inflation with exponentially small tensor-to-scalar ratio,” *Phys. Rev. D* **110**, L061302 (2024), arXiv:2405.13881 [astro-ph.CO].
- [71] Shamit Kachru, Renata Kallosh, Andrei D. Linde, and Sandip P. Trivedi, “De Sitter vacua in string theory,” *Phys. Rev. D* **68**, 046005 (2003), arXiv:hep-th/0301240.
- [72] Fedor L. Bezrukov and Mikhail Shaposhnikov, “The Standard Model Higgs boson as the inflaton,” *Phys. Lett. B* **659**, 703–706 (2008), arXiv:0710.3755 [hep-th].
- [73] By adding a light spectator field to single-field models, the PBH-forming dynamics more closely resemble the well-studied physics of hybrid inflation [44–52]: a sharp turn in field space combined with a brief phase of tachyonic growth seeds PBH formation.
- [74] Sam Young, Ilia Musco, and Christian T. Byrnes, “Primordial black hole formation and abundance: contribution from the non-linear relation between the density and curvature perturbation,” *JCAP* **11**, 012 (2019), arXiv:1904.00984 [astro-ph.CO].
- [75] Alex Kehagias, Ilia Musco, and Antonio Riotto, “Non-Gaussian Formation of Primordial Black Holes: Effects on the Threshold,” *JCAP* **12**, 029 (2019), arXiv:1906.07135 [astro-ph.CO].
- [76] Albert Escrivà, Cristiano Germani, and Ravi K. Sheth, “Universal threshold for primordial black hole formation,” *Phys. Rev. D* **101**, 044022 (2020), arXiv:1907.13311 [gr-qc].
- [77] V. De Luca, G. Franciolini, and A. Riotto, “On the Primordial Black Hole Mass Function for Broad Spectra,” *Phys. Lett. B* **807**, 135550 (2020), arXiv:2001.04371 [astro-ph.CO].
- [78] Ilia Musco, Valerio De Luca, Gabriele Franciolini, and Antonio Riotto, “Threshold for primordial black holes. II. A simple analytic prescription,” *Phys. Rev. D* **103**, 063538 (2021), arXiv:2011.03014 [astro-ph.CO].
- [79] Shu-Lin Cheng, Da-Shin Lee, and Kin-Wang Ng, “Power spectrum of primordial perturbations during ultra-slow-roll inflation with back reaction effects,” *Phys. Lett. B* **827**, 136956 (2022), arXiv:2106.09275 [astro-ph.CO].
- [80] Jason Kristiano and Jun’ichi Yokoyama, “Constraining Primordial Black Hole Formation from Single-Field Inflation,” *Phys. Rev. Lett.* **132**, 221003 (2024), arXiv:2211.03395 [hep-th].
- [81] Jason Kristiano and Jun’ichi Yokoyama, “Note on the bispectrum and one-loop corrections in single-field inflation with primordial black hole formation,” *Phys. Rev. D* **109**, 103541 (2024), arXiv:2303.00341 [hep-th].
- [82] Sayantan Choudhury, Mayukh R. Gangopadhyay, and M. Sami, “No-go for the formation of heavy mass Primordial Black Holes in Single Field Inflation,” *Eur. Phys. J. C* **84**, 884 (2024), arXiv:2301.10000 [astro-ph.CO].
- [83] Sayantan Choudhury, Sudhakar Panda, and M. Sami, “PBH formation in EFT of single field inflation with sharp transition,” *Phys. Lett. B* **845**, 138123 (2023), arXiv:2302.05655 [astro-ph.CO].
- [84] Shu-Lin Cheng, Da-Shin Lee, and Kin-Wang Ng, “Primordial perturbations from ultra-slow-roll single-field inflation with quantum loop effects,” *JCAP* **03**, 008 (2024), arXiv:2305.16810 [astro-ph.CO].
- [85] Leonardo Senatore and Matias Zaldarriaga, “On Loops in Inflation,” *JHEP* **12**, 008 (2010), arXiv:0912.2734 [hep-th].

- [86] Leonardo Senatore and Matias Zaldarriaga, “On Loops in Inflation II: IR Effects in Single Clock Inflation,” *JHEP* **01**, 109 (2013), [arXiv:1203.6354 \[hep-th\]](#).
- [87] Guilherme L. Pimentel, Leonardo Senatore, and Matias Zaldarriaga, “On Loops in Inflation III: Time Independence of zeta in Single Clock Inflation,” *JHEP* **07**, 166 (2012), [arXiv:1203.6651 \[hep-th\]](#).
- [88] Leonardo Senatore and Matias Zaldarriaga, “The constancy of  $\zeta$  in single-clock Inflation at all loops,” *JHEP* **09**, 148 (2013), [arXiv:1210.6048 \[hep-th\]](#).
- [89] Kenta Ando and Vincent Vennin, “Power spectrum in stochastic inflation,” *JCAP* **04**, 057 (2021), [arXiv:2012.02031 \[astro-ph.CO\]](#).
- [90] A. Riotto, “The Primordial Black Hole Formation from Single-Field Inflation is Still Not Ruled Out,” (2023), [arXiv:2303.01727 \[astro-ph.CO\]](#).
- [91] Hassan Firouzjahi, “One-loop corrections in power spectrum in single field inflation,” *JCAP* **10**, 006 (2023), [arXiv:2303.12025 \[astro-ph.CO\]](#).
- [92] Hayato Motohashi and Yuichiro Tada, “Squeezed bispectrum and one-loop corrections in transient constant-roll inflation,” *JCAP* **08**, 069 (2023), [arXiv:2303.16035 \[astro-ph.CO\]](#).
- [93] Hassan Firouzjahi and Antonio Riotto, “Primordial Black Holes and loops in single-field inflation,” *JCAP* **02**, 021 (2024), [arXiv:2304.07801 \[astro-ph.CO\]](#).
- [94] Gabriele Franciolini, Antonio Iovino, Junior., Marco Taoso, and Alfredo Urbano, “Perturbativity in the presence of ultraslow-roll dynamics,” *Phys. Rev. D* **109**, 123550 (2024), [arXiv:2305.03491 \[astro-ph.CO\]](#).
- [95] Gianmassimo Tasinato, “Large  $|\eta|$  approach to single field inflation,” *Phys. Rev. D* **108**, 043526 (2023), [arXiv:2305.11568 \[hep-th\]](#).
- [96] Angelo Caravano, Keisuke Inomata, and Sébastien Renaux-Petel, “Inflationary Butterfly Effect: Nonperturbative Dynamics from Small-Scale Features,” *Phys. Rev. Lett.* **133**, 151001 (2024), [arXiv:2403.12811 \[astro-ph.CO\]](#).
- [97] Angelo Caravano, Gabriele Franciolini, and Sébastien Renaux-Petel, “Ultraslow-roll inflation on the lattice: Backreaction and nonlinear effects,” *Phys. Rev. D* **111**, 063518 (2025), [arXiv:2410.23942 \[astro-ph.CO\]](#).
- [98] Keisuke Inomata, Matteo Braglia, Xingang Chen, and Sébastien Renaux-Petel, “Questions on calculation of primordial power spectrum with large spikes: the resonance model case,” *JCAP* **04**, 011 (2023), [Erratum: *JCAP* **09**, E01 (2023)], [arXiv:2211.02586 \[astro-ph.CO\]](#).
- [99] Ioanna D. Stamou, “Exploring critical overdensity thresholds in inflationary models of primordial black holes formation,” *Phys. Rev. D* **108**, 063515 (2023), [arXiv:2306.02758 \[astro-ph.CO\]](#).
- [100] Ioanna D. Stamou, “Large curvature fluctuations from no-scale supergravity with a spectator field,” *Phys. Lett. B* **855**, 138798 (2024), [arXiv:2404.02295 \[astro-ph.CO\]](#).
- [101] Ioanna Stamou, “Mechanisms for Producing Primordial Black Holes from Inflationary Models beyond Fine-Tuning,” *Universe* **10**, 241 (2024), [arXiv:2404.14321 \[astro-ph.CO\]](#).
- [102] A. Wilkins and A. Cable, “Spectators no more! how even unimportant fields can ruin your primordial black hole model,” *Journal of Cosmology and Astroparticle Physics* **2024**, 026 (2024).
- [103] Tomotaka Kuroda, Atsushi Naruko, Vincent Vennin, and Masahide Yamaguchi, “Primordial black holes from a curvaton: the role of bimodal distributions,” (2025), [arXiv:2504.09548 \[astro-ph.CO\]](#).
- [104] Scott Dodelson and Lam Hui, “A Horizon ratio bound for inflationary fluctuations,” *Phys. Rev. Lett.* **91**, 131301 (2003), [arXiv:astro-ph/0305113](#).
- [105] Andrew R Liddle and Samuel M Leach, “How long before the end of inflation were observable perturbations produced?” *Phys. Rev. D* **68**, 103503 (2003), [arXiv:astro-ph/0305263](#).
- [106] Mustafa A. Amin, Mark P. Hertzberg, David I. Kaiser, and Johanna Karouby, “Nonperturbative Dynamics Of Reheating After Inflation: A Review,” *Int. J. Mod. Phys. D* **24**, 1530003 (2014), [arXiv:1410.3808 \[hep-ph\]](#).
- [107] Jessica L. Cook, Emanuela Dimastrogiovanni, Damien A. Easson, and Lawrence M. Krauss, “Reheating predictions in single field inflation,” *JCAP* **04**, 047 (2015), [arXiv:1502.04673 \[astro-ph.CO\]](#).
- [108] Jerome Martin, Christophe Ringeval, and Vincent Vennin, “Information Gain on Reheating: the One Bit Milestone,” *Phys. Rev. D* **93**, 103532 (2016), [arXiv:1603.02606 \[astro-ph.CO\]](#).
- [109] Rouzbeh Allahverdi *et al.*, “The First Three Seconds: a Review of Possible Expansion Histories of the Early Universe,” *Open J. Astrophys.* **4** (2020), 10.21105/astro.2006.16182, [arXiv:2006.16182 \[astro-ph.CO\]](#).
- [110] P. A. R. Ade *et al.* (Planck), “Planck 2015 results. XX. Constraints on inflation,” *Astron. Astrophys.* **594**, A20 (2016), [arXiv:1502.02114 \[astro-ph.CO\]](#).
- [111] Mafalda Dias, Jonathan Frazer, David J. Mulryne, and David Seery, “Numerical evaluation of the bispectrum in multiple field inflation—the transport approach with code,” *JCAP* **12**, 033 (2016), [arXiv:1609.00379 \[astro-ph.CO\]](#).
- [112] David J. Mulryne and John W. Ronayne, “PyTransport: A Python package for the calculation of inflationary correlation functions,” *J. Open Source Softw.* **3**, 494 (2018), [arXiv:1609.00381 \[astro-ph.CO\]](#).
- [113] David H. Lyth and Andrew R. Liddle, *The Primordial Density Perturbation* (Cambridge University Press, New York, 2009).

## Appendix: Model Parameters and Observables

The model parameters used in the previous figures are reported in Table A1 for the PBHA model of Eq. (10) and in Table AIII for the PBHB model of Eq. (11). The evolution of the background quantities  $\epsilon$  and  $\omega$ , and of the perturbations  $\mathcal{R}_k$  and  $\mathcal{S}_k$ , are shown for model PBHB in Figs. A1 and A2; these correspond to the evolution of those quantities depicted in Figs. 2 and 3 for the PBHA model.

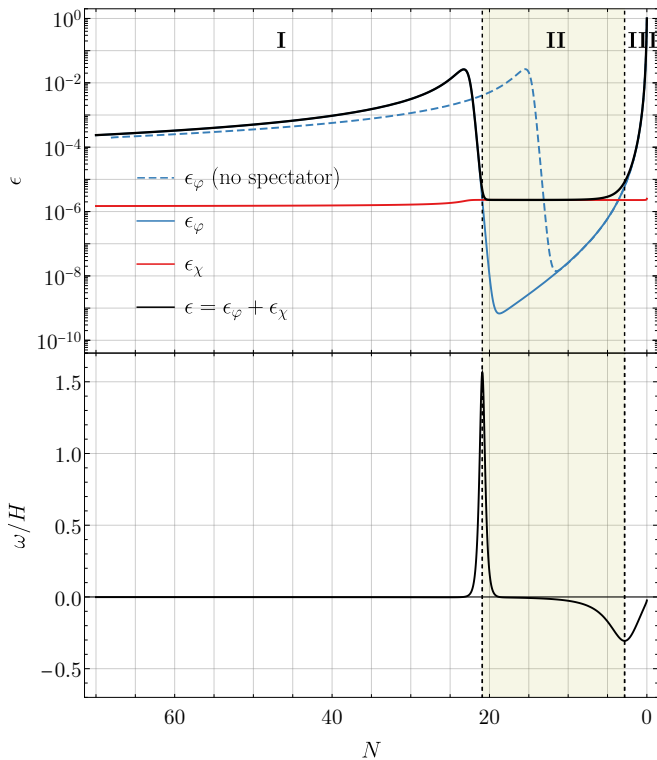


FIG. A1. Evolution of the background quantities as functions of the number of e-folds  $N$  before the end of inflation, for the PBHB model of Eq. (11). Model parameters are reported in Table AIII. *Top panel*: Slow-roll parameter  $\epsilon$  and its components; for comparison, the evolution of  $\epsilon$  for the spectator-less case is also shown. *Bottom panel*: Turn rate pseudoscalar  $\omega/H$ , showing the change in trajectory of the background field system; the dashed vertical lines correspond to the extrema of  $\omega$ . *Both panels*: The highlighted ‘phase II’ is delimited by the turns and corresponds to the field trajectory being aligned with the  $\chi$  direction; during this time,  $\epsilon_\chi \gg \epsilon_\phi$ .

The CMB observables calculated for each of the PBHA and PBHB models considered throughout are summarized in Tables AII and AIV, respectively. Their definitions are given below, and their best-fit observational values are reported in Table AV.

The time at which the comoving CMB pivot scale,  $k_{\text{CMB}} = 0.05 \text{ Mpc}^{-1}$ , first crosses the Hubble radius is

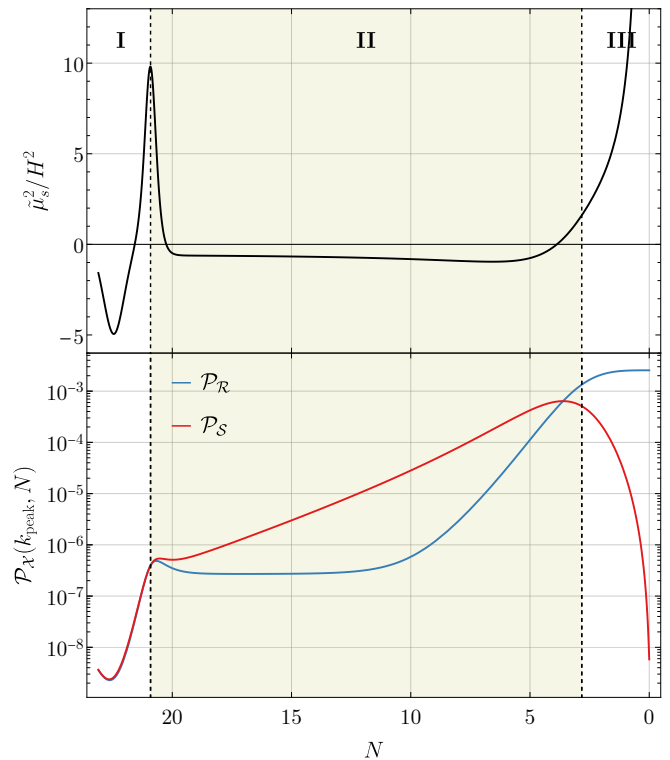


FIG. A2. Evolution of the perturbations for the PBHB model of Eq. (11), with parameters reported in Table AIII. *Top panel*: Isocurvature effective mass  $\tilde{\mu}_s^2$ ; the tachyonic instability is highlighted in phase II. *Bottom panel*: Spectra of curvature ( $\mathcal{R}$ ) and isocurvature ( $\mathcal{S}$ ) perturbations for a mode  $k_{\text{peak}}$  that exits the Hubble radius  $\sim 30$  e-folds before the end of inflation. The isocurvature mode undergoes tachyonic growth during phase II before transferring power to the curvature perturbation while  $\omega \neq 0$  at the transition to phase III.

found through the standard relation [104, 105]

$$N_{\text{CMB}} \simeq 62 + \frac{1}{4} \ln \left( \frac{\rho_{\text{CMB}}^2}{3M_{\text{Pl}}^6 H_e^2} \right) + \frac{1 - 3w_{\text{reh}}}{12(1 + w_{\text{reh}})} \ln \left( \frac{\rho_{\text{rad}}}{\rho_e} \right) \simeq 56 \pm 5,$$

where  $\rho_{\text{CMB}}$  is the energy density of the field system at the CMB scale,  $\rho_{\text{rad}}$  is the energy density when the Universe achieves radiation-dominated evolution after inflation and reheating (see, e.g., Refs. [106–109]),  $H_e$  and  $\rho_e$  are evaluated at the end of inflation, and  $w_{\text{reh}} \in \{-1/3, +1\}$  is the equation of state of reheating. (The range  $\pm 5$  reflects uncertainty in the duration of reheating.) The central value corresponds to instant reheating, with  $w_{\text{reh}} = 1/3$ .

Experimental efforts to observe the CMB phenomenologically parametrise the primordial power spectrum of curvature perturbations  $\mathcal{P}_{\mathcal{R}}(k)$  as [110]

$$\mathcal{P}_{\mathcal{R}}(k) \equiv A_s \left( \frac{k}{k_{\text{CMB}}} \right)^{n_s - 1 + \frac{1}{2} \alpha_s \ln \left( \frac{k}{k_{\text{CMB}}} \right)}, \quad (\text{A1})$$

where  $A_s = \mathcal{P}_{\mathcal{R}}(k_{\text{CMB}})$  is the scalar amplitude of modes that exit the Hubble radius at the CMB scale  $k_{\text{CMB}}$ ,  $n_s$  is the scalar spectral index (i.e. the departure of the slope of  $\mathcal{P}_{\mathcal{R}}$  from unity), and  $\alpha_s$  is the running of the scalar spectral index. The latter are defined as

$$n_s \equiv 1 + \left. \frac{d \ln \mathcal{P}_{\mathcal{R}}(k)}{d \ln k} \right|_{k=k_{\text{CMB}}}, \quad (\text{A2})$$

$$\alpha_s \equiv \left. \frac{d n_s}{d \ln k} \right|_{k=k_{\text{CMB}}}. \quad (\text{A3})$$

The tensor-to-scalar ratio is defined as the ratio between the amplitudes of tensor and scalar perturbations at the CMB pivot scale,  $r \equiv A_t/A_s$ . Here,  $A_t \equiv \mathcal{P}_t(k_{\text{CMB}})$ , the power spectrum of the tensor modes  $h_k$ .

The primordial isocurvature fraction is defined as [42]

$$\beta_{\text{iso}}(k) \equiv \frac{\mathcal{P}_{\mathcal{S}}(k)}{\mathcal{P}_{\mathcal{R}}(k) + \mathcal{P}_{\mathcal{S}}(k)}, \quad (\text{A4})$$

and is expected to be small in these models, since isocurvature modes  $\mathcal{S}_k$  decay at the end of the inflationary evolution, when  $\tilde{\mu}_s > 0$  (see bottom panels of Figs. 3 and A2). We evaluate  $\beta_{\text{iso}}$  at the CMB pivot scale, corresponding to the scale  $k_{\text{mid}}$  in Ref. [42].

The non-Gaussianity of the model is calculated using the publicly available Python code `PyTransport` [111, 112]. We find that non-Gaussianity is  $< \mathcal{O}(1)$  for both the single-field and spectator models, and that the bispectrum is peaked in the orthogonal configuration. Note that the modes  $k_{\text{PBH}}$  never contribute to this measure since they correspond to much smaller scales than

those probed by CMB data, even in the squeezed limit. Planck 2018 CMB data probes  $\ell$  and hence  $k \approx \ell/\eta_0$  [113], where  $\eta_0 \simeq 14000$  Mpc is the particle horizon, over a range of  $\mathcal{O}(10^{-3})$ , corresponding to  $\approx 7$  e-folds of inflation. This in turn restricts the range of  $k$  that can be measured in the CMB (including non-Gaussianity) to  $k \ll k_{\text{PBH}}$ . We quote the values of  $f_{\text{NL}}^{\text{ortho}}$  in Tables AII and AIV, which were found to be larger than  $f_{\text{NL}}^{\text{equil}}$  and  $f_{\text{NL}}^{\text{local}}$ . (For model  $\chi$ -PBHB-var, which exhibits the largest non-Gaussianity,  $f_{\text{NL}}^{\text{ortho}} = 0.66$  while  $f_{\text{NL}}^{\text{equil}} = 0.20$  and  $f_{\text{NL}}^{\text{local}} = 0.55$ .)

Primordial black holes form from the gravitational collapse of overdensities after the end of inflation. In order for PBHs to form, the dimensionless power spectrum must exceed the threshold  $\mathcal{P}_{\mathcal{R}}(k_{\text{peak}}) \geq 10^{-3}$  [14, 74–78], where  $k_{\text{peak}}$  is the comoving wavenumber at which  $\mathcal{P}_{\mathcal{R}}(k)$  reaches its maximum value. The resulting population of PBHs forms with a mass distribution whose peak depends on  $k_{\text{PBH}} \simeq k_{\text{peak}}$ . The characteristic mass is proportional to the mass contained within a Hubble radius at the time of collapse,  $M_{\text{PBH},f} = \gamma M_H(t_f)$ , where  $\gamma \simeq 0.2$  is an efficiency factor [5], the subscript f refers to the time of formation, and  $M_H(t) \equiv 4\pi\rho(t)/(3H^3(t))$ . This can be recast as [33]

$$\frac{M_{\text{PBH},f}}{30 M_{\odot}} \simeq \left( \frac{\gamma}{0.2} \right) \left( \frac{g_*(T_f)}{106.75} \right)^{-\frac{1}{6}} \left( \frac{k_{\text{PBH}}}{3.2 \times 10^5 \text{ Mpc}^{-1}} \right)^{-2}. \quad (\text{A5})$$

In this work, we take  $\gamma = 0.2$ , consider the effective number of relativistic degrees of freedom to be  $g_*(T_f) = 106.75$ , and we translate this mass into grams using  $M_{\odot} \simeq 2.0 \times 10^{33}$  g.

Model	$V_0 [M_{\text{Pl}}^4]$	$\varphi_d [M_{\text{Pl}}]$	$m_\chi [M_{\text{Pl}}]$	$\chi_i [M_{\text{Pl}}]$
PBHA-fid	$8.3 \times 10^{-11}$	2.18812	—	—
PBHA-var	$6.6 \times 10^{-11}$	$2.18812 \times (1 - 10^{-3})$	—	—
$\chi$ -PBHA-fid	$8.3 \times 10^{-11}$	2.18812	$1 \times 10^{-8}$	5
$\chi$ -PBHA-var	$8.9 \times 10^{-11}$	$2.18812 \times (1 - 10^{-3})$	$3 \times 10^{-7}$	11

TABLE AI. Values of the parameters considered for the PBHA model. For each case, we fix the values  $M = 1/2$ ,  $A = 1.17 \times 10^{-3}$ , and  $\sigma = 1.59 \times 10^{-2}$  (in units of  $M_{\text{Pl}}$ ), and always consider the initial value  $\varphi_i = 3.5 M_{\text{Pl}}$  and  $\dot{\varphi}_i = 0$  for the inflaton. The reference model PBHA-fid uses the same parameters considered in Ref. [34], while PBHA-var shifts the parameter  $\varphi_d \rightarrow \varphi_{d,\text{fid}} \times (1 - 10^{-3})$ . The corresponding models  $\chi$ -PBHA-fid and  $\chi$ -PBHA-var include the effect of a spectator field.

Model	$A_s$	$n_s$	$\alpha_s$	$r$	$\beta_{\text{iso}}$	$f_{\text{NL}}^{\text{ortho}}$	$M_{\text{PBH}} [\text{g}]$	$V_S/V_{\text{PBH}}$	$m_\chi/H$
PBHA-fid	$2.11 \times 10^{-9}$	0.9647	$-8.2 \times 10^{-4}$	0.003	—	0.25	$7.3 \times 10^{21}$	—	—
PBHA-var	$2.09 \times 10^{-9}$	0.9694	$-6.2 \times 10^{-4}$	0.002	—	0.25	—	—	—
$\chi$ -PBHA-fid	$2.11 \times 10^{-9}$	0.9647	$-8.2 \times 10^{-4}$	0.003	$1.8 \times 10^{-4}$	0.25	$8.2 \times 10^{21}$	$2 \times 10^{-5}$	0.002
$\chi$ -PBHA-var	$2.09 \times 10^{-9}$	0.9634	$-8.7 \times 10^{-4}$	0.003	$2.1 \times 10^{-4}$	0.25	$8.1 \times 10^{23}$	0.06	0.06

TABLE AII. Observables for all the parameter sets considered for the PBHA model (as defined in Table AI). CMB scales exit at  $N_\star = 56$ . The non-Gaussianities are peaked in the orthogonal configuration, and  $\beta_{\text{iso}}$  is taken at the scale  $k = 0.05 \text{ Mpc}^{-1}$  (i.e.  $k_{\text{mid}}$  in Ref [42]). The ‘spectator-ness’ measures  $V_S/V_{\text{PBH}}$  and  $m_\chi/H$  are calculated at the time  $t_{\text{CMB}}$ , when CMB scales first exit the Hubble radius. We point out that  $M_{\text{PBH}}$  for the  $\chi$ -PBHA-var model is just above the threshold for the asteroid-mass range (see Table AV); this is due to the choice of the fiducial model PBHA-fid of Ref. [34], which already produces PBHs at the boundary of the asteroid-mass range. By choosing different values of the model parameters, the power spectra of Fig. 1 could all be shifted rightwards, producing PBHs within the asteroid-mass range.

Model	$\lambda$	$v [M_{\text{Pl}}]$	$m_\chi [M_{\text{Pl}}]$	$\chi_i [M_{\text{Pl}}]$
PBHB-fid	$1.16 \times 10^{-6}$	0.19669	—	—
PBHB-var	$9.10 \times 10^{-7}$	$0.19669 \times (1 - 4 \times 10^{-3})$	—	—
$\chi$ -PBHB-fid	$1.16 \times 10^{-6}$	0.19669	$1 \times 10^{-8}$	5
$\chi$ -PBHB-var	$1.20 \times 10^{-6}$	$0.19669 \times (1 - 4 \times 10^{-3})$	$2 \times 10^{-7}$	8

TABLE AIII. Values of the parameters considered for the PBHB model. For each case, we fix the values  $a = 0.719527$  and  $b = 1.500016$ , and always consider the initial value  $\varphi_i = 3 M_{\text{Pl}}$  for the inflaton. The reference model PBHB-fid reproduces the results introduced in Ref. [21], modified to be in agreement with the latest CMB constraints and producing PBHs in the asteroid-mass range, while PBHB-var shifts the parameter  $v \rightarrow v_{\text{fid}} \times (1 - 4 \times 10^{-3})$ . The corresponding models  $\chi$ -PBHB-fid and  $\chi$ -PBHB-var include the effect of a spectator field.

Model	$A_s$	$n_s$	$\alpha_s$	$r$	$\beta_{\text{iso}}$	$f_{\text{NL}}^{\text{ortho}}$	$M_{\text{PBH}} [\text{g}]$	$R_V$	$m_\chi/H$
PBHB-fid	$2.10 \times 10^{-9}$	0.9599	$-1.8 \times 10^{-3}$	0.005	—	0.66	$1.1 \times 10^{17}$	—	—
PBHB-var	$2.10 \times 10^{-9}$	0.9665	$-8.2 \times 10^{-4}$	0.004	—	0.66	—	—	—
$\chi$ -PBHB-fid	$2.10 \times 10^{-9}$	0.9598	$-1.3 \times 10^{-3}$	0.005	$3.7 \times 10^{-4}$	0.66	$1.1 \times 10^{17}$	$9 \times 10^{-6}$	0.002
$\chi$ -PBHB-var	$2.10 \times 10^{-9}$	0.9593	$-1.0 \times 10^{-3}$	0.005	$3.3 \times 10^{-4}$	0.66	$5.8 \times 10^{17}$	0.009	0.03

TABLE AIV. Observables for all the parameter sets considered for the PBHB model (as defined in Table AIII). CMB scales exit at  $N_\star = 56$ . The non-Gaussianities are peaked in the orthogonal configuration, and  $\beta_{\text{iso}}$  is taken at the scale  $k = 0.05 \text{ Mpc}^{-1}$  (i.e.  $k_{\text{mid}}$  in Ref [42]). The ‘spectator-ness’ measures  $V_S/V_{\text{PBH}}$  and  $m_\chi/H$  are calculated at the time  $t_{\text{CMB}}$ , when CMB scales first exit the Hubble radius.

$A_s [\times 10^{-9}]$	$n_s$	$\alpha_s$	$r$	$\beta_{\text{iso}}$	$f_{\text{NL}}^{\text{ortho}}$	$M_{\text{PBH}} [\text{g}]$
$2.10 \pm 0.03$	$0.9665 \pm 0.0038$	$-0.0045 \pm 0.0067$	$< 0.037$	$< 0.001$	$-38 \pm 24$	$[10^{17} - 10^{23}]$

TABLE AV. Constraints from Planck 2018 CMB data [40–43] and PBH constraints [8–17].